



LAWRENCE
LIVERMORE
NATIONAL
LABORATORY

An Electrical Micro-Heater Technique for High-Pressure and High-Temperature Diamond Anvil Cell Experiments

S. T. Weir, D. D. Jackson, S. Falabella, G. Samudrala, Y. K. Vohra

October 13, 2008

Review of Scientific Instruments

Disclaimer

This document was prepared as an account of work sponsored by an agency of the United States government. Neither the United States government nor Lawrence Livermore National Security, LLC, nor any of their employees makes any warranty, expressed or implied, or assumes any legal liability or responsibility for the accuracy, completeness, or usefulness of any information, apparatus, product, or process disclosed, or represents that its use would not infringe privately owned rights. Reference herein to any specific commercial product, process, or service by trade name, trademark, manufacturer, or otherwise does not necessarily constitute or imply its endorsement, recommendation, or favoring by the United States government or Lawrence Livermore National Security, LLC. The views and opinions of authors expressed herein do not necessarily state or reflect those of the United States government or Lawrence Livermore National Security, LLC, and shall not be used for advertising or product endorsement purposes.

An Electrical Micro-Heater Technique for High-Pressure and High-Temperature
Diamond Anvil Cell Experiments

S.T. Weir [†], D.D. Jackson [†][◇], S. Falabella [†], G. Samudrala [★], and Y.K. Vohra [★]

[†] Lawrence Livermore National Laboratory
Livermore, CA 94550

[★] Department of Physics
University of Alabama at Birmingham
Birmingham, AL 35294-1170

Abstract

Small electrical heating elements have been lithographically fabricated onto the culets of “designer” diamond anvils for the purpose of performing high-pressure and high-temperature experiments on metals. The thin-film geometry of the heating elements makes them very resistant to plastic deformation during high pressure loading, and their small cross-sectional area enables them to be electrically heated to very high temperatures with relatively modest currents (≈ 1 Amp). The technique also offers excellent control and temporal stability of the sample temperature. Test experiments on gold samples have been performed for pressures up to 21 GPa and temperatures of nearly 2000K.

[◇] Present Address: Senergen Devices, Inc., Fremont, CA 94538

I. Introduction

The generation of well controlled high-pressure and high-temperature conditions is essential for many areas of research in physics, materials science, and geophysics. Examples include the study of high-pressure and high-temperature phase diagrams [1,2], the synthesis of new metastable materials [3,4], and the study of the physical and chemical properties of geological materials under extreme conditions [5,6,7]. Diamond anvil cells (DAC) are capable of generating pressures of up to several hundred GPa at room-temperature, but achieving conditions of high pressures and high temperatures under well controlled and well characterized conditions remains problematic. For temperatures up to approximately 1200 °C, electrical resistance heaters can be used to heat either the entire DAC, or just the region surrounding the diamond anvils and gasket [8]. This approach ensures that the temperature of the sample is very uniform, and that the temperature can be precisely controlled and measured. However, this method cannot be used for temperatures much higher than 1200 °C because diamond starts to graphitize and other parts of the DAC, including the pressure gasket, start to weaken.

DAC sample temperatures much greater than 1200 °C are possible if the heating is localized to the sample itself so that the diamond anvils and the rest of the DAC remain relatively cool. Laser heating of the sample through the diamond anvils is commonly used for this purpose, and sample temperatures of several thousand degrees have been reached in this way [9,10]. Localized heating of DAC samples presents numerous difficulties, however. Temperature gradients in the vicinity of the sample are necessarily large, and this may affect the temperature uniformity of the sample. Also, since diamond has an extremely high thermal conductivity, samples must be insulated from the anvils by an appropriate thermal insulating layer (e.g., argon, alumina) which does not chemically react with the sample. Additional complications which may affect data quality include possible temporal variations in the laser heating beam and thermal drifting of the beam alignment.

An alternative method for locally heating the sample is internal resistive heating [1,11,12,13], in which a large electrical current is passed through the sample itself, or through an electrical heater next to the sample. This technique is attractive because it offers excellent temporal stability of the sample temperature, as well as the possibility of achieving high temperature uniformity throughout the sample volume. Recently, C-S Zha, et. al. [14], developed an internal resistive heating technique which enabled them to measure the P-V-T equation of state of platinum to 80 GPa and 1900 K. Internal resistive heating techniques tend to be very difficult to implement, however. The sample as well as the tiny electrical heating element must be precisely placed on a very small diamond culet. Furthermore, since the pressure gasket and the sample region of a DAC undergo significant plastic strain as the DAC is pressurized, which causes deformation and eventual failure of the internal resistive heating circuit as the loading increases, internal resistive heating experiments have always been severely pressure-limited in comparison to laser heating DAC experiments.

In this paper we describe a new method for performing internal resistive heating experiments utilizing specially fabricated “designer” diamond anvils with electrical circuits that are lithographically fabricated directly onto the diamond anvils [15,16]. This approach offers precise control over the layout and geometry of the heating circuit and

sample as well as good temperature uniformity over the sample volume. Also, because the thin-film heating circuit undergoes very little plastic deformation under high pressure loading, it is potentially capable of operating at very high pressures.

II. Electrical Heating Arrangement

A key feature of our internal resistive heating technique is the use of “designer” diamond anvils which have the important electrical heating circuit components directly integrated into the anvils themselves. Designer diamond anvils are fabricated from standard 1/3 carat, brilliant-cut diamond anvils by lithographically fabricating electrical circuits onto them, and then encasing the circuits in a layer of epitaxial diamond by a chemical vapor deposition (CVD) process. Details have been described previously [15,16]. Due to the epitaxial nature of the diamond film growth, the completed diamond anvils are essentially single crystal diamonds, but with electrical circuits now running through their interiors. These designer diamond anvils have been successfully used in experiments to Mbar pressures [17,18,19]. Furthermore, because their internal circuitry can be easily altered, designer diamond anvils are readily adaptable to various types of high pressure experiments, such as electrical conductivity [15,18] and magnetic susceptibility [16,20]. In this paper we describe the modification of these anvils to electrically heat high-pressure samples to very high temperatures.

Internal resistive heating techniques must satisfy a number of difficult experimental requirements. Considerable electrical power must be delivered to and dissipated by a very small heating element precisely located at the center of diamond culet with a typical diameter of 300 μm or less. Also, the sample must be surrounded by sufficient thermal insulation so that the dissipated power can effectively heat the sample to very high temperatures. Finally, the entire circuit must be mechanically robust under DAC pressure loading so that electrical continuity is maintained at high pressure, without an open-circuit or closed-circuit condition developing due to either a break in the wires or an electrical short from the heating circuit to the metal pressure gasket. This is a difficult problem because the pressure gasket and the sample chamber inevitably undergo large amounts of plastic deformation as the DAC is pressurized.

To address these requirements, we modified our diamond anvils into the design shown in Figure 1. In this anvil, eight thin-film tungsten electrodes, each 10 μm wide and 0.5 μm thick, extend from electrical connection pads on the sides of the anvil up to the culet of the anvil. The electrodes are encased in a diamond film layer averaging about 20 μm in thickness, and the ends of these electrodes emerge from the diamond near the center of the culet.

In the center of the electrical probe pattern, a small circular pit 6-8 μm deep and 30-35 μm in diameter was plasma etched into the surface of the diamond. An rf-driven, hollow-cathode plasma source of Lawrence Livermore National Laboratory (LLNL) design was used for the etching. The source provides a high-density oxygen plasma in a 3 mm diameter plume at the exit of the source. With a 13.56 MHz rf-power input of only 27 watts, we were able to achieve an etch rate of 9 $\mu\text{m}/\text{hour}$. Since the diamond is removed by a chemical reaction with the oxygen, any non-reactive impurities on the surface will reduce the local etch rate and lead to a rough texture on the bottom of the

etched pit. To minimize this, a non-specific etch (i.e., an argon rf-discharge on the substrate) was performed prior to the reactive etch.

The pit was then densely packed with a fine alumina powder (Saint Gobain, 0.05 μm alumina powder) using a mechanical chuck which firmly pressed the powder against the diamond anvil. Excess alumina was then gently brushed off, leaving just the packed powder in the pit. This alumina filled pit serves as a thermal insulation layer for the electrical heating element which was subsequently fabricated on top of it.

At this stage, the electrical heating element is fabricated onto the culet of the anvil by lithographic patterning followed by sputter depositing a layer of tungsten 0.5 μm thick. The resulting pattern makes electrical contact to six of the electrodes, then extends across the alumina filled pit in order to make contact to the remaining two electrodes (Figure 1). The pattern then continues down the side of the diamond anvil. During electrical heating operation, five of the six electrodes on the right side of the anvil are used to deliver electrical current to the heating element, while the sixth electrode, together with one of the two electrodes on the opposite side of the heating element, is used to monitor the voltage drop across the heating element. The thin-film circuit pattern then extends off to the left side of the anvil, where it makes electrical contact to the metal gasket which serves as the return path for the electrical heating circuit.

The resulting anvil and circuit are well suited for achieving high temperatures under high pressure conditions. By connecting five of the electrodes together and driving electrical current through them in parallel, the circuit resistance is reduced from approximately 150 Ω (typical resistance of one electrode) to about 30 Ω (resistance of five electrodes in parallel), which enables higher currents to be sent through the anvil without overheating it. Also, by using a thin-film heating element rather than a small, cylindrical wire, the cross-sectional area of the heating element can be made very small, which translates into higher current densities and more electrical power dissipation per unit length of the heating element. For example, previous internal resistive heating experiments typically used wire diameters of 10 to 25 μm [2,12], which corresponds to a cross-sectional area of about 78 to 490 μm^2 . In comparison, a 10 μm wide, 0.5 μm thick thin-film heating element has a cross-sectional area of just 5 μm^2 , or at least 15-times smaller. Thus, for a given electrical current, the thin-film heating element described dissipates roughly 15-times more electrical power per unit length than a 10 μm diameter wire made of the same metal. As a result, temperatures of well over 1000 $^{\circ}\text{C}$ can be reached with relatively modest currents of up to about 1 Ampere, as opposed to the much higher currents required for larger wires.

Another attractive feature of this high-pressure heating method is that the circuit performs very well under high pressures with no noticeable deformation. Although the heating circuit is fabricated on top of a relatively weak alumina thermal insulation layer instead of onto diamond, very little plastic deformation of the layer occurs because the alumina layer is effectively ‘trapped’ in an extremely rigid diamond cavity and is therefore unable to undergo any significant amount of large-scale plastic flow. In addition, the very low profile of the thin-film heating circuit keeps the entire circuit close to the strong, rigid diamond anvil and away from regions of the sample chamber and gasket which undergo large amounts of plastic strain during pressure loading. An electrical circuit having a higher profile which extended, say, 10 μm or more above the surface of the diamond anvil would be subjected to much more plastic strain during

pressure loading, leading to possible damage and destruction of the circuit. On the other hand, the low profile of the actual thin-film heating circuit appears to help make it quite resistant to deformation, and we have never observed any noticeable change in either the geometry or the position of the heating circuit under high pressures.

As mentioned earlier, two of the designer anvil's eight electrodes, one on each side of the heating element, are reserved for monitoring the voltage drop across the heating element. This monitoring is very important for proper control of the current through the heating element. As pointed out by others [13], the thermal stability characteristics of an electrical heating circuit depend on whether the circuit is driven by a constant-current power supply or a constant-voltage power supply. If a constant current I is being driven through a heating element, then the power P dissipated by the heating element is directly proportional to its resistance R ($P=I^2 \cdot R$). Since the resistance of most metals tends to increase with temperature, an increase in temperature results in an increase in power dissipation which, in turn, causes a further increase in temperature. Under some conditions, this positive feedback effect may even be large enough to cause a thermal runaway. But even if it is not, significant positive feedback may make precise temperature control very difficult and overly sensitive to the input current. If, on the other hand, a constant voltage V is applied to the heating element, then the power P dissipated by the heating element is inversely proportional to the resistance R ($P=V^2/R$). In this case, an increase in temperature results in a decrease in power dissipation, i.e., the feedback effect is negative, not positive, and the heating behavior tends to be more stable.

When using a designer anvil to electrically heat samples, the circuit setup is complicated by the fact that the resistance of the diamond encased electrical leads ($\approx 30 \, \Omega$) is much greater than that of the heating element itself ($\approx 1 \, \Omega$ at room temperature). Thus, even when a constant-voltage source is used to drive the designer anvil, from the perspective of the heating element it is being driven not by a constant-voltage source, but by a quasi-constant current source [21]. Consequently, the control and heating stability problems associated with constant-current sources may affect heating experiments using designer anvils even when a constant-voltage source is used.

We solve this problem by means of an electronic control circuit which actively monitors the voltage directly across the heating element (V_{heater}), and automatically adjusts the total voltage V_{total} applied to the designer anvil in order to keep the voltage across the heating element fixed to a specified value (Figure 2). In operation, we specify the desired heating element voltage by adjusting a dial on our control circuit, and the control circuit then increases (or decreases) the total voltage V_{total} until the measured heating element voltage V_{heater} matches the desired value. In this way, we are able to exercise precise control over the heating element voltage (V_{heater}) despite the presence of the relatively large resistance in series with the heating element, and ensure stable operation of the heating element at high temperatures.

III Circuit Operation and Detection of Melting at High Pressure

We have demonstrated the operation of our high-pressure and -temperature technique using thin-film samples of gold which are directly sputtered onto the heating element through a photoresist mask. A typical sample size is a $10 \, \mu\text{m}$ diameter, $0.5 \, \mu\text{m}$ thick circular dot sputtered onto the middle of a $10 \, \mu\text{m}$ wide heating element (Figure 3).

Samples consisting of 5 μm diameter, 0.5 μm thick dots sputtered onto 5 μm wide heating elements have also been used. The gold sputtering target had a purity of greater than 99.9%. Small inclusions of argon in the sputtered film are believed to be present at the less than 1% level. However, since argon is inert and forms no known compounds with gold, the presence of small argon inclusions is not believed to affect the melting temperature of gold.

Sputter deposition ensures good thermal and electrical contact between the sample and the heating element. Good temperature uniformity is achieved in the axial direction because the thickness of the sample is only about 1 μm or less, which is much smaller than the thicknesses of the alumina insulating layers above and below the sample. In the lateral directions, the constant width and thickness of the heating element across the center of the alumina filled pit promotes uniform power dissipation and temperatures throughout this region. This is supported by 2D thermal simulations which indicate modest temperature variations over the cross-sectional area of the heating element of 2% with 5 μm wide heaters and 5% with 10 μm wide heaters (Figure 4).

The electrical contact between a sputtered metal sample and the tungsten heating element enables the heating circuit to be also used as a sample diagnostic. Sudden changes in the electrical resistivity of the sample due to a phase transition can be detected as changes in the current-vs-voltage behavior of the composite heating element. This is illustrated in Figure 5, which shows how the combination of the heating element and the attached sample can be modeled as a series-parallel electrical circuit, with a total resistance which changes in response to changes in the resistivity of the sample. Electrical resistance changes are particularly useful for detecting solid-to-liquid phase transitions, because these transitions tend to be associated with especially large changes in resistivity. The resistivities of most elemental metals, for instance, abruptly increase by about a factor of two when they melt [22].

To prepare a DAC for these high-pressure and –temperature experiments, the designer diamond anvil with the gold sample was matched and aligned to another diamond anvil with a 300 μm flat culet. The pressure gasket was made of spring steel and had an initial thickness of about 80 μm and an initial sample chamber diameter of 110 μm . The sample chamber was filled with packed alumina powder (Saint Gobain, 0.05 μm) in order to provide thermal insulation between the heating element and the diamond anvil opposite to it. Several ruby chips with a size of ≈ 10 μm were placed close to the sample to act as a pressure marker, and the DAC was sealed.

To detect sample melting at high pressure, the sample pressure was first increased to some value, and then the sample temperature was raised by increasing the heater voltage and current by means of the control circuit described earlier. The temperature was measured using blackbody spectroradiometry which observed the tungsten heater through the table of the designer anvil. The emissivity of tungsten was assumed to be independent of wavelength. The pressure was determined by ruby fluorescence measurements [23] taken immediately before and after heating and averaged.

Figure 6 shows a typical current-voltage (I-V) plot. The current and voltage are seen to smoothly increase until encountering an abrupt discontinuity at a current of about 530 mA. We identify this discontinuity as signaling the melting of the high pressure gold sample. The upward curvature of the I-V data is due to the fact that the resistivity of tungsten increases with increasing temperature, an effect not included in the simple

model of Figure 5. Associating the discontinuity in the I-V curve with the melting of the gold sample is supported by a number of facts: (1) the temperature at which the discontinuity occurs when the sample is at low pressures agrees well with the known zero pressure melting temperature of gold ($T_{\text{melt}}=1337\text{K}$); (2) discontinuities in the I-V curve are never observed when using tungsten heating elements having no gold samples on them, so the discontinuities are in fact associated with the gold sample and not some other feature of the heating circuit or DAC; (3) the direction of the observed discontinuities always corresponds to an increase in resistance, which is consistent with the sample melting interpretation. If, for example, the discontinuity were due to the sample passing through its recrystallization temperature, the resistance would be expected to abruptly decrease, not increase. On the basis of all these facts, we believe that the observed I-V discontinuities are indeed associated with the melting of the gold samples. Figure 7 shows some preliminary results of some gold melting experiments using the designer anvil microheater technique.

IV Future Measurements

The micro-heater technique described here has a number of attractive features for high-pressure and –temperature studies of metals. The temporal stability of the sample temperature is excellent, and the control circuit allows very precise adjustments of the sample temperature to be made. Good temperature uniformity is achieved in the axial direction because of the small thickness of the sample ($\approx 1\text{ }\mu\text{m}$), its direct thermal contact to the heating element, and the relatively large thicknesses of the alumina insulating layers ($>6\text{ }\mu\text{m}$) on either side of the sample. Also, the constant width and thickness of the heating element across the center of the alumina pit helps promote uniform power dissipation and temperatures. Finally, because of the very small size of the thin-film heating element and the sample, as well as the amount of insulation around the heating element, only modest amounts of electrical power need to be dissipated by the heating element in order to take it to high temperatures. As seen in the current-vs-voltage data of Figure 6, a power dissipation in the heating element of only about 1 Watt ($\approx 500\text{ mA} \times 2000\text{ mV}$) is needed to heat it to a temperature of 1920 K.

The unique thin-film geometry of the microheater technique offers a number of attractive features for possible future development and exploitation. For example, since the thin-film sample and the thin-film tungsten directly under the sample share the same temperature and pressure, one future possibility is to use the thin-film tungsten as an *in situ* pressure marker for use at high-pressure and high-temperature. This could be accomplished by using a focused x-ray beam to simultaneously record diffraction lines from both the metal sample and the tungsten heater.

Another future possibility is to use two microheater designer anvils together in a DAC in order to heat a sample from opposite sides in a manner analogous to double-sided laser heating. This would remove the current restriction on thin metal film samples, and allow many other types of samples to be studied. Microheater elements with much larger areas (e.g., $30\text{ }\mu\text{m} \times 30\text{ }\mu\text{m}$ or more) would be required in order to ensure good temperature uniformity in the sample sandwiched between the microheater elements. Also, the control circuits would need to be modified to simultaneously operate two microheater elements and adjust their power levels so that their temperatures are equal.

Acknowledgements

We thank C. Aracne and D. Ruddie for technical support. This work performed under the auspices of the U.S. Department of Energy by Lawrence Livermore National Laboratory under Contract DE-AC52-07NA27344.

Figure Captions:

Figure 1. Schematic diagrams of a microheater designer anvil. (a) A side-view schematic showing the designer anvil with a thin-film heating element on its culet and an alumina thermal insulator layer below the heating element. Alumina is also packed into the pressure gasket above the heating element in order to thermally insulate it from the upper diamond anvil. (b) A top-view schematic of a microheater designer anvil showing the eight diamond encased electrodes (the view of the two electrodes on the left side is mostly masked by the heating element pattern). One side of the heating element pattern is connected to six of the electrodes, five of which transport electrical current to the narrow heating bridge running across the alumina layer. The left side of the heating element pattern connects to two of the electrodes and then extends off to the left and makes electrical contact to the metal pressure gasket, which acts as the return electrical path.

Figure 2. (a) Schematic diagram for the overall setup of a microheater designer anvil circuit. A control circuit monitors the voltage drop across the heating element and automatically adjusts the power supply voltage in order to ensure that the voltage across the heating element remains fixed to a specified value. (b) A detailed circuit schematic of the control circuit. Current to the designer anvil is regulated by a MOSFET transistor (IRF520) which in turn is controlled by voltage input from two LM324 op-amps. The lower op-amp amplifies the small voltage drop across the heating element, and the upper op-amp compares the amplified voltage with the specified control voltage.

Figure 3. A photograph of a microheater designer anvil showing a 10 μm diameter, 0.5 μm thick gold dot which has been sputter deposited onto the center of a 10 μm wide tungsten heating element. Electrical current (I) for the heating element is delivered by the five electrodes indicated, and the voltage drop (V) across the heating element is monitored by two electrodes on opposite sides of the element. The inset shows a microheater designer anvil in operation at a pressure of 10 GPa and a temperature of approximately 1500K.

Figure 4. A 2D thermal simulation of the heating element showing the temperature contours. The heating element in this simulation is 5 μm wide and 1 μm thick. The alumina filled pit below the heating element is 30 μm in diameter and 5 μm thick. The two diamond anvils were both heat-sunked to 20 $^{\circ}\text{C}$ (to represent external cooling), and ohmic power dissipation in the heating element was modeled by generating heat uniformly throughout the volume of the heating element. The thermal conductivities of diamond, tungsten, and the 0.05 μm packed alumina powder were taken to be 2000, 178, and 1 $\text{W/m}^{\circ}\text{C}$, respectively. Simulation was performed using the FEHT Finite Element Heat Transfer program (F-Chart Software).

Figure 5. (a) A schematic of an equivalent series-parallel circuit of the composite heating element consisting of a tungsten heating element with a thin-film metal sample on it. The resistors R_{Sample} and R_{Tungsten} represent the resistances of small length segments of the sample and the tungsten heater, respectively. The resistance of the sample (R_{Sample}) can be expected to increase by a significant amount when the sample melts (about a 2x increase

in resistivity for most elemental metals passing through the solid-to-liquid phase transition). (b) A schematic plot representing the current-vs-voltage behavior expected as a result of sample melting. A sudden change in the current-vs-voltage data indicates the melting of the sample.

Figure 6. A current-vs-voltage (I-V) plot taken at a gold sample pressure of 21.0 GPa. The melting of the gold sample is marked by the sudden change in the current-vs-voltage curve at a temperature of $T=1920\text{K}$. The upward curvature in the I-V data is due to the increasing resistivity of tungsten with increasing temperature.

Figure 7. A plot showing the preliminary results of gold melting experiments using the designer anvil microheater technique (red squares). Also shown are previous high-pressure gold melting data taken by Zha and Bassett [13] (black circles), and by Mirwald and Kennedy [24] (white squares).

¹ L. Liu and W.A. Bassett, *J. Geophys. Res.* **80**, 3777 (1975).

² H.K. Mao, P.M. Bell, and C. Hadidiacos, *High-Pressure Research in Mineral Physics*, M.H. Manghnani and Y. Syono, eds., pp. 135-138 (1987).

³ M.I. Erements, A.G. Gavriluk, I.A. Trojan, D.A. Dzivenko, and R. Boehler, *Nature Materials* **3**, 558 (2004).

⁴ V. Iota, C.S. Yoo, and H. Cynn, *Science* **283**, 1510 (1999).

⁵ A. Lacam, M. Madon, and J.P. Poirier, *Nature* **288**, 155 (1980).

⁶ L. Ming and W.A. Bassett, *Science* **187**, 66 (1975).

⁷ R.J. Hemley, P.M. Bell, and H.K. Mao, *Science* **237**, 605 (1987).

⁸ D. Schiferl, et. al., in *High Pressure Research in Mineral Physics* (ed. M.H. Manghnani, and Y. Syono, American Geophysical Union, Washington, DC), pp. 75-83 (1987)

⁹ Y. Meng, G. Shen, and H.K. Mao, *J. Phys. Cond. Mat.* **18**, S1097 (2006).

¹⁰ M. Kunz, W.A. Caldwell, L. Miyagi, and H-R Wenk, *Rev. Sci. Instrum.* **78**, 63907 (2007).

¹¹ H.K. Mao, P.M. Bell, and C. Hadidiacos, in *High Pressure Research in Mineral Physics* (ed. M.H. Manghnani, and Y. Syono, American Geophysical Union, Washington, DC), pp. 135-138 (1987)

¹² R. Boehler, M. Nicol, M.L. Johnson, in *High Pressure Research in Mineral Physics* (ed. M.H. Manghnani, and Y. Syono, American Geophysical Union, Washington, DC), pp. 173-176 (1987)

¹³ C-S Zha and W.A. Bassett, *Rev. Sci. Instrum.* **74**, 1255 (2003).

¹⁴ C-S Zha, et. al., *J. Appl. Phys.* **103**, 54908 (2008).

¹⁵ S.T. Weir, J. Akella, C. Aracne-Ruddle, Y.K. Vohra, and S.A. Catledge, *Appl. Phys. Lett.* **77**, 3401 (2000).

¹⁶ D.D. Jackson, C. Aracne-Ruddle, V. Malba, S.T. Weir, S.A. Catledge, and Y.K. Vohra, *Rev. Sci. Instrum.* **74**, 2467 (2003).

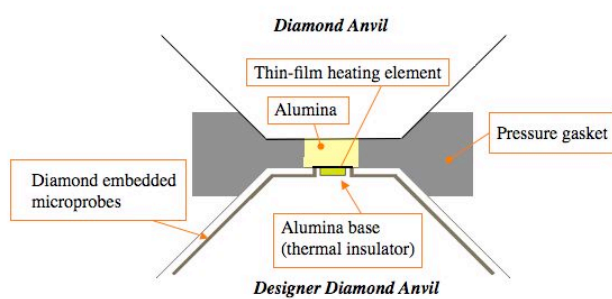
¹⁷ N. Velisavljevic, K. MacMinn, Y.K. Vohra, and S.T. Weir, *Appl. Phys. Lett.* **84**, 927 (2004).

-
- ¹⁸ J.R. Patterson, C.M. Aracne, D.D. Jackson, V. Malba, S.T. Weir, P.A. Baker, and Y.K. Vohra, *Phys. Rev. B* **69**, 220101 (2004).
- ¹⁹ J-F Lin, S.T. Weir, D.D. Jackson, W.J. Evans, Y.K. Vohra, W. Qiu, and C-S Yoo, *Geophys. Res. Lett.* **34**, L16305 (2007).
- ²⁰ D.D. Jackson, V. Malba, S.T. Weir, P.A. Baker, and Y.K. Vohra, *Phys. Rev. B* **71**, 184416 (2005).
- ²¹ The current through the heating element is insensitive to small changes in the resistance of the heating element because of the presence of the much larger $\approx 30\ \Omega$ probe resistance in series with it. The current (I) through the heating element is equal to the total applied voltage V_{total} across the designer anvil divided by the total resistance or $I = V_{\text{total}}/(30\ \Omega + R_{\text{heater}}) \approx V_{\text{total}}/30\ \Omega$. Thus, the current I through the heating element is approximately constant and insensitive to changes in the heater resistance R_{heater} when $R_{\text{heater}} \ll 30\ \Omega$.
- ²² A.M. Rosenfeld, and M.J. Stott, *Phys. Rev. B* **42**, 3406 (1990).
- ²³ H.K. Mao, P.M. Bell, J.W. Shaner, and D.J. Steinberg, *J. Appl. Phys.* **49**, 3276 (1978).
- ²⁴ P.W. Mirwald, and G.C. Kennedy, *J. Geophys. Res.* **84**, 6750 (1979).

Figures:

Figure 1

(a)



(b)

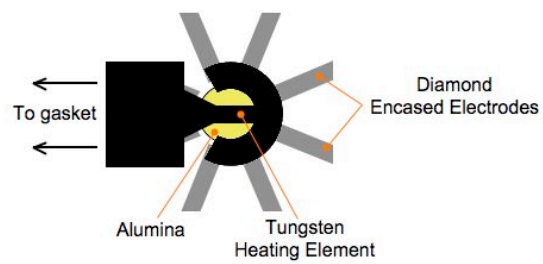


Figure 2a

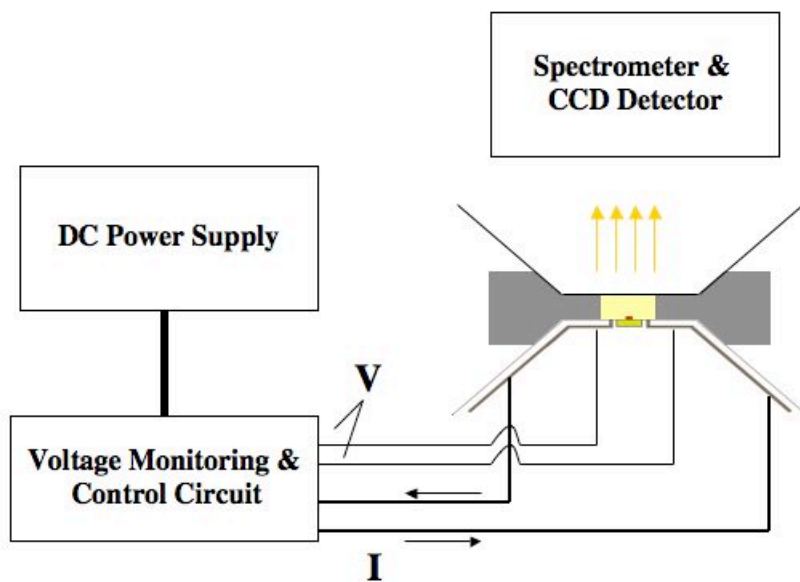


Figure 2b

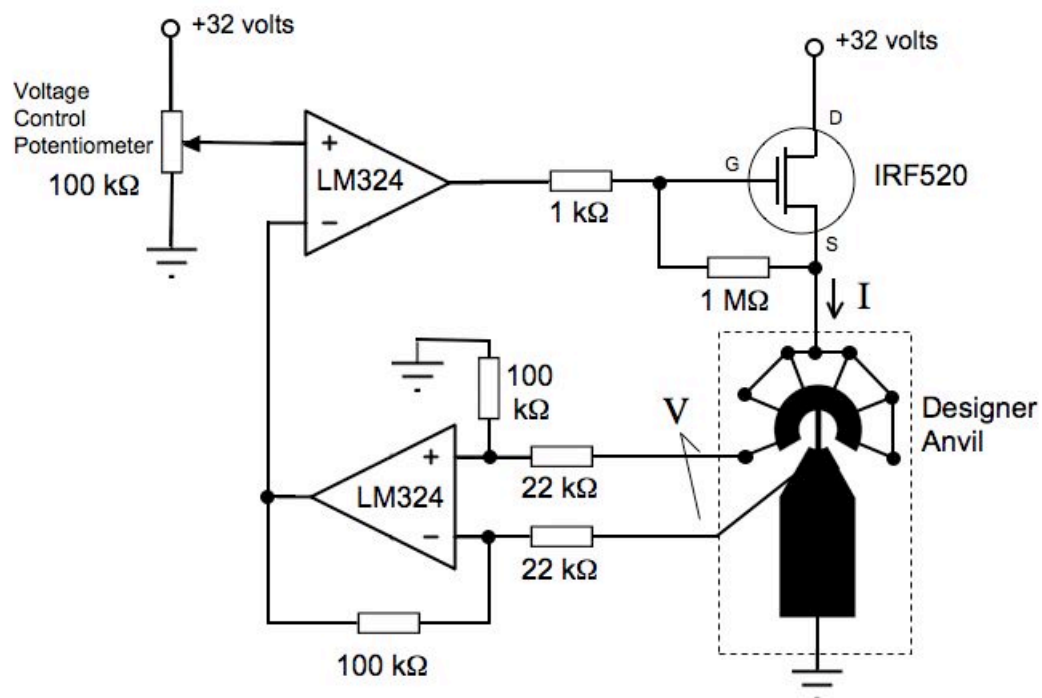


Figure 3

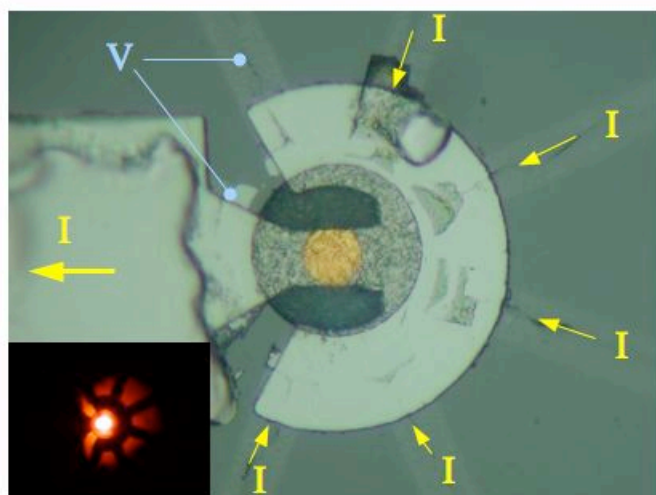


Figure 4

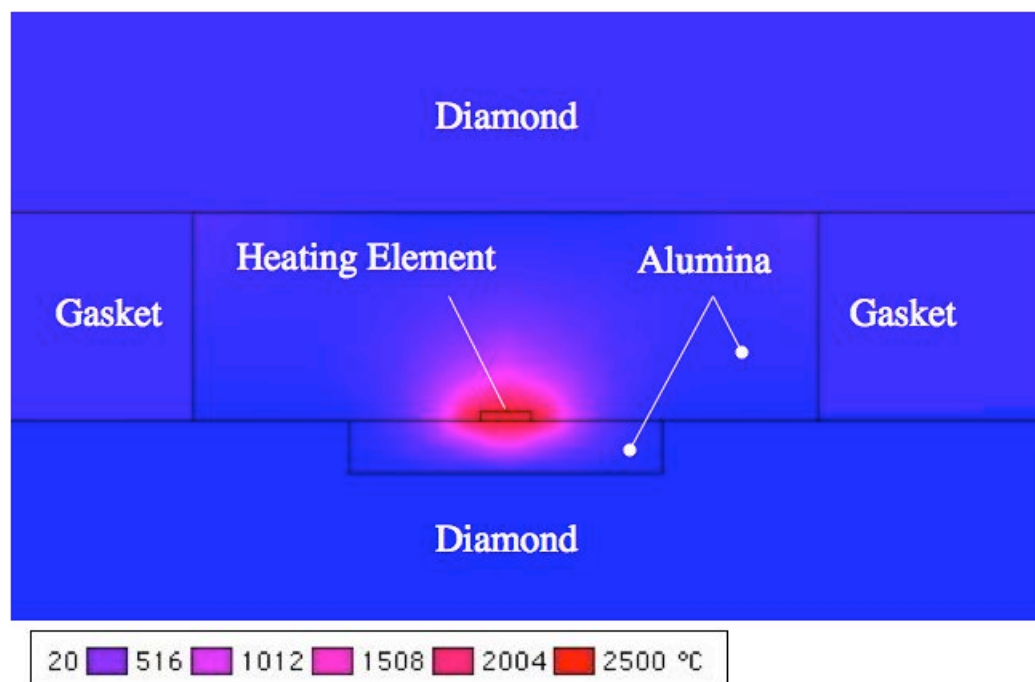


Figure 5

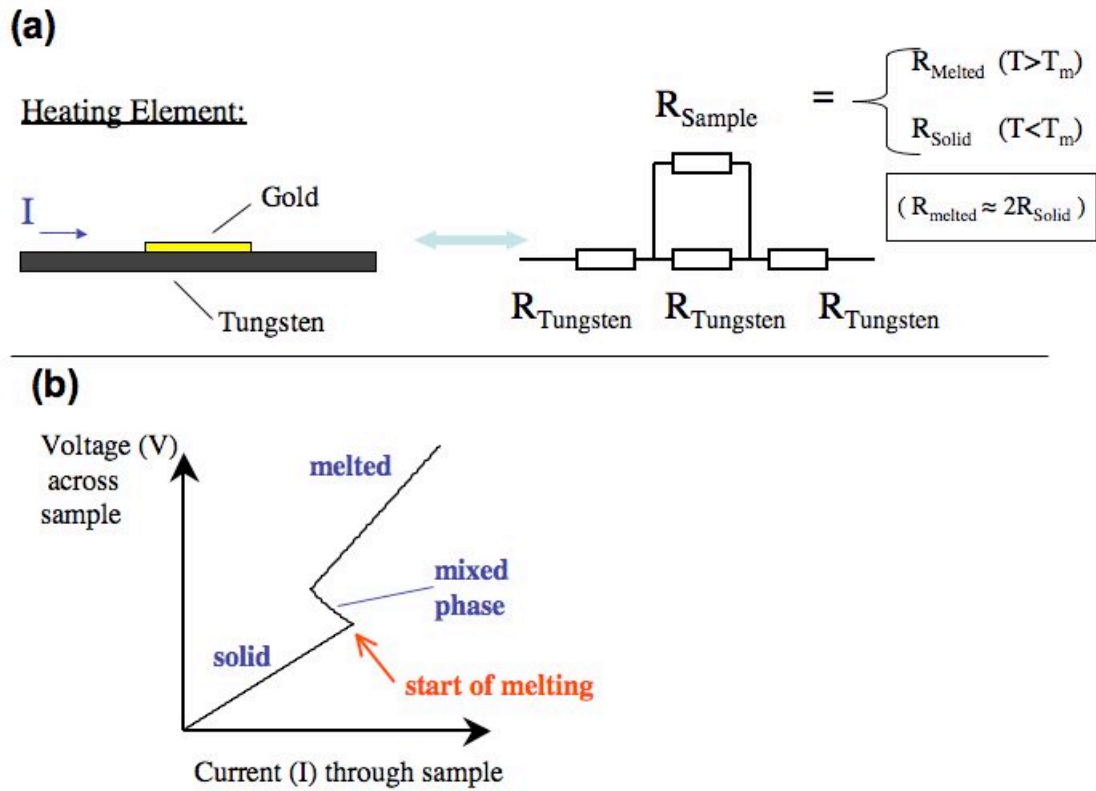


Figure 6

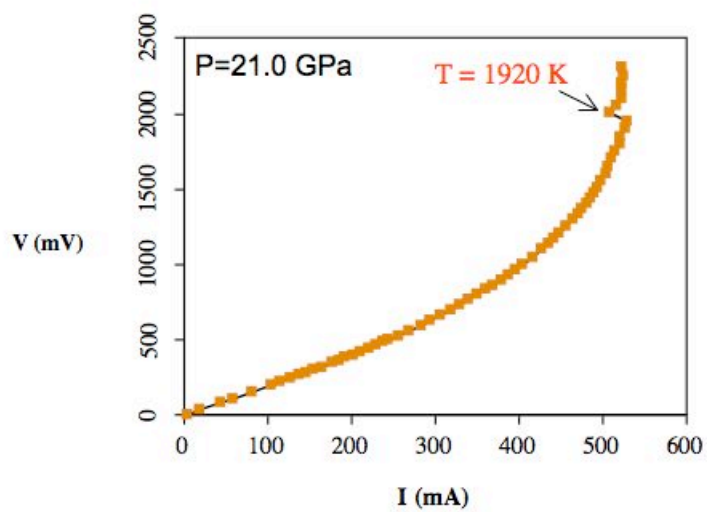


Figure 7

